Oxytocin receptor expression patterns in the human brain across development

Jaroslav Rokicki [1,2.3], Tobias Kaufmann [1,4], Ann-Marie G. De Lange [1,5,6], Dennis van der Meer [1,7], Shahram Bahrami [1,2], Alina M. Sartorius [1,2], Unn K. Haukvik [1,3], Nils Eiel Steen[1], Emanuel Schwarz [8], Dan J. Stein [9], Terje Nærland [10,11], Ole A. Andreassen [1,11], Lars T. Westlye [1,2,11], and Daniel S. Quintana [1,2,11*]

[1] NORMENT Centre for Psychosis Research, Division of Mental Health and Addiction, University of Oslo and Oslo University Hospital, Oslo, Norway

[2] Department of Psychology, University of Oslo, Oslo, Norway

[3] Centre of Research and Education in Forensic Psychiatry, Oslo University Hospital, Oslo, Norway

[4] Department of Psychiatry and Psychotherapy, University of Tübingen, Germany

[5] LREN, Centre for Research in Neurosciences - Department of Clinical Neurosciences, CHUV and University of Lausanne, Lausanne, Switzerland

[6] Department of Psychiatry, University of Oxford, Oxford, UK

[7] School of Mental Health and Neuroscience, Faculty of Health, Medicine and Life Sciences, Maastricht University, Maastricht, The Netherlands

[8] Central Institute of Mental Health, Department of Psychiatry and Psychotherapy, Medical Faculty Mannheim, Heidelberg University, Mannheim, Germany

[9] SAMRC Unit on Risk & Resilience in Mental Disorders, Department of Psychiatry and Neuroscience Institute, University of Cape Town, Cape Town, South Africa

[10] NevSom, Department of Rare Disorders, Oslo University Hospital, Oslo, Norway

[11] KG Jebsen Centre for Neurodevelopmental Disorders, University of Oslo, Oslo, Norway

* Corresponding author: Daniel S. Quintana (daniel.quintana@psykologi.uio.no)

Abstract

Background: Oxytocin plays a vital role in social behavior and homeostatic processes, with animal models indicating that oxytocin receptor (*OXTR*) expression patterns in the brain influence behavior and physiology. However, the developmental trajectory of *OXTR* gene expression is unclear, which is considerable knowledge gap as many psychiatric illnesses emerge early in life and genes tend to be differentially regulated across development.

Methods: We calculated spatiotemporal expression patterns for 16660 genes in the human brain using transcriptome data from 57 donors across the lifespan. Next, we explored the evolutionary origin of these patterns using a comparative gene expression dataset from 38 macaque donors. Finally, we determined the functional significance of *OXTR* spatiotemporal co-expression patterns via the annotation of genetic associations with psychiatric and body composition phenotypes.

Results*: OXTR* expression in the brain accelerated before birth with a peak in early childhood and *OXTR* expression was highly correlated with dopamine receptor D2 expression across development. These gene expression patterns were not observed in a comparative macaque sample, suggesting they might be evolutionarily new features. In addition, a network of genes strongly spatiotemporally coupled with *OXTR* was enriched in schizophrenia, cognitive, and body composition phenotypes, with elements of this gene network having undergone positive selection in humans but not macaques.

Conclusions: These results demonstrate that oxytocin signaling plays an important role in a diverse set of psychological and physiological processes across the lifespan. Identifying a critical window of *OXTR* expression in the brain, together with associated genes, may help illuminate our understanding of disease etiology.

Introduction

Oxytocin is an evolutionarily ancient neuromodulator that facilitates mammalian social behavior and metabolic regulatory processes (1,2). Oxytocin is primarily produced in the hypothalamus, for both central and peripheral release (3), and binds to oxytocin receptors that are located throughout the brain and the periphery (1,2). Both the experimental manipulation of *OXTR* expression levels and *OXTR* gene knockout can have a dramatic effect on behavior and physiology (4,5). Thus, the identification of *OXTR* expression patterns in the human brain can help identify the functional relevance of the oxytocin signaling system. We recently mapped the voxel-wise density of *OXTR* expression across the adult human brain, finding increased expression in subcortical and olfactory regions (6). Moreover, the location of *OXTR* expression was highly correlated with dopaminergic gene expression and closely matched the neural activity patterns observed in anticipatory, appetitive, and aversive mental states, along with homeostatic regulation. Research has also shown that compared to control donors, *OXTR* expression in the dorsolateral prefrontal cortex is increased in donors diagnosed with mood disorders (7) and reduced in the temporal cortex of donors diagnosed with schizophrenia (8).

While the *OXTR* gene expression pattern in the adult human brain has been described (6), little is known about the evolution and functional relevance of *OXTR* gene expression and *OXTR* gene co-expression patterns across the lifespan. This is a critical knowledge gap, as genes are differentially regulated across the brain over development (9) and disturbances in neural development contribute to the genesis of mental illness (10). Supporting the clinical relevance of spatially and temporally distinct aberrations, neurotypical postmortem brain tissue from the ventral pallidum (VP) and nucleus basalis of Maynert has been reported to have higher *OXTR* binding than postmortem VP tissue from autistic donors, and an early childhood peak of *OXTR* binding that was observed in VP tissue from neurotypical donors was absent in VP tissue from autistic donors (11).

The oxytocin system emerges very early in the course of mammalian development. Oxytocin has been detected prenatally during the neurogenesis period of fetal brain

development (12) and magnocellular oxytocin neurons only mature a few weeks postnatally (13). Oxytocin system dysregulation during early development also plays an important role in behavior later in life (14). For example, oxytocin concentrations in cerebrospinal fluid (CSF) are significantly higher in mother-reared rhesus monkeys compared to nursery reared monkeys (15) and increased maternal behaviors are associated with higher central *OXTR* expression levels in rat pups (16). In humans, women with a history of child abuse also demonstrate reduced CSF oxytocin (17), highlighting how the early environment can influence later oxytocin system functioning.

Mental and physical illnesses tend to follow specific developmental trajectories. Thus, the identification of a critical window of oxytocin system expression in the brain, together with associated genes, may illuminate our understanding of mental illnesses. Research has identified patterns of increased *OXTR* expression in non-human mammals during either infancy, childhood, or adulthood, compared to other lifespan periods (18). However, it is not known which of these characteristic patterns are observed in humans and the functional significance of observed patterns. In addition, some aspects of oxytocin's role in behavior are sexually dimorphic, but it is unclear whether sex differences in gene expression patterns are related to these effects. Therefore, there is a need to characterize typical oxytocin pathway system development, to determine whether expression patterns are stable over development, and to identify critical periods.

Here we identified the spatiotemporal distribution patterns of *OXTR* expression and gene expression interactions in human brain tissue from the prenatal period to late adulthood. We also examined the evolutionary conservation of *OXTR* expression patterns by replicating our first analysis using macaque *OXTR* expression data and extended this analysis by identifying the evolutionary origin of genes with strong spatiotemporal associations with *OXTR* expression. Finally, we explored the functional significance of genes with a strong spatiotemporal association with *OXTR* by assessing if this geneset was enriched of in various GWAS of psychiatric, cognitive, and body composition phenotypes.

Methods

Spatiotemporal expression of the oxytocin pathway in humans

To better understand the functional relevance of spatiotemporal gene co-expression patterns across the lifespan and relevance to common human traits and diseases, we determined *OXTR* expression patterns, along with all available protein coding genes, across sixteen regions of the human brain from the prenatal stage (5.7 pre-conception weeks) to 82 years of age in 57 donors (26 females, 31 males). We used genome-wide exon-level transcriptome data available from the Gene Expression Omnibus database (https://www.ncbi.nlm.nih.gov/geo; series GSE25219) as a proxy of *OXTR* receptor density (19). Human gene expression data was converted from months and years into days for the purposes of analysis.

Gene expression values for sixteen brain regions were visualized across the lifespan using two approaches. The first approach illustrates absolute change in gene expression patterns across the lifespan for sixteen brain regions. We analyzed data from sixteen brain regions in humans: primary motor cortex (M1C), dorsolateral prefrontal cortex (DFC), ventrolateral prefrontal cortex (VFC), orbital frontal cortex (OFC), primary somatosensory cortex (S1C), inferior parietal cortex (IPC), primary auditory cortex (A1C), caudal superior temporal cortex (STC), inferolateral temporal cortex (ITC), primary visual cortex (V1C), medial prefrontal cortex (MFC), hippocampus (HIP), striatum (STR), amygdala (AMY), mediodorsal nucleus of the thalamus (MD), and cerebellar cortex (CBC). The expression values were smoothed via a logarithmic scale using locally weighted least squares regression, then demeaned and scaled (i.e., divided by the standard deviation), yielding a data frame with expression values converted to Z-scores per brain region of interest. Thus, the mean expression of a given brain region across the lifespan is zero. In these "ribbon plots", Z-values are stacked on top of each other and scaled again by number of regions, so when a single region (or group of regions) demonstrates increased expression relative to other life periods, the peaks will be higher.

Our second visualization approach provides complementary information via a "heat plot", with the key difference of age normalized expression values. This provides a stronger emphasis on expression changes in specific brain regions, rather than overall expression across the brain. For example, a value of 0.25 in the cerebellum during adolescence means that at this developmental stage 25% of gene expression occurs in the cerebellum compared to 75% in the remaining 15 regions at the same age period. Expression levels are shown by colors instead of ribbon height.

Lifespan correlation between genes

We have previously shown using a voxel-wise approach in the adult brain that *OXTR* expression is highly correlated with the expression of a selection of oxytocinergic, dopaminergic, muscarinic acetylcholine, and opioid pathway genes (6). Thus, we assessed whether this geneset also had a strong spatiotemporal relationship with *OXTR*. To calculate the lifespan correlation for two given genes, we first we calculated Spearman's *r* correlation coefficient within each donor. Then, we interpolated calculated points on a logarithmic scale using locally weighted least squares regression (with a span of 0.4 for the human data and a span of 0.7 for the macaque data). To evaluate the lifespan average, we calculated the mean of the interpolated line, which we labeled the "trajectory" mean. By using this approach, each life period receives an equal weighting. To complement this measure, we also presented the arithmetic mean of all points, so that each donor was weighted equally. To assess the specificity of the correlation between two selected genes, we also plotted the distribution of the correlation between a gene of interest against all remaining genes (16659 for humans and 19049 for macaques), marking the location of the correlated genes of interest.

Using correlation data between genes, we generated a 14×14 correlation matrix reflecting the spatiotemporal Spearman's correlation for each donor for each mRNA map pair, using the mean of fitted trajectories in lower-left triangle, so that each time period gets equal

weight and mean of all points in the upper-right triangle, so that each subject gets equal weight. As per our previous analysis (6), we used the following genes (Oxytocin pathway set: *OXTR*, *CD38*, *OXT*; Dopaminergic set: *DRD1*, *DRD2*, *DRD3*, *DRD4*, *DRD5*, *COMT*, and *DAT1*; muscarinic acetylcholine set: *CRHM1*, *CRHM2*, *CRHM3*, *CRHM4*, and *CRHM5*; opioid set: *OPRM1*, *OPRD1*, *OPRK1*, and *AVPR1A*, which is a vasopressin signaling gene). We used Ward's hierarchical clustering to identify highly correlated groups of genes within this geneset.

The evolutionary origin of genes spatiotemporally associated with OXTR

To explore the degree to which spatiotemporal patterns of oxytocin pathway expression across human development reflect a recent evolutionary adaption, rhesus macaque (*macaca mulatta*) gene expression data from post-mortem brain tissue was extracted from the National Institute of Health Blueprint Non-human primate (NIH Blueprint NHP) atlas (http://www.blueprintnhpatlas.org/). This atlas provides data for central gene expression across six prenatal stages (40, 50, 70, 80, 90, and 120 embryonic days) and four postnatal periods (neonate, infant, juvenile, and young adult). We assumed pregnancy to last 40 weeks for humans and 166.5 embryonic days for macaques. Spatiotemporal *OXTR* expression patterns in macaques were generated using the same methods as described above as humans (i.e., a ribbon plot to best illustrate change across time and heat plot to best illustrate changes in specific brain regions). For the macaque analysis, twenty brain regions were analyzed.

While comparing gene expression patterns between humans and macaques is instructive, this only represents a comparison within a relatively short evolutionary period for two species. In contrast, phylostratigraphy can facilitate the identification of the evolutionary origin of genes using data across the entire evolutionary tree (20). As gene modules with high co-expression in the brain are related to molecular functions (21), we created a geneset containing the genes with the 100 strongest spatiotemporal correlations with *OXTR*. For our

phylostratigraphy analysis, a phylostratigraphic map from Domazet-Lošo and Tautz (22), with gene age inferences combined with human gene expression data from five ontogenetic stages (prenatal, infant, child, adolescent, adult) extracted from the BrainSpan atlas (http://brainspan.org) for evolutionary transcriptomics via the 'myTAI' R package (23). For each brain region, a transcriptional age index (TAI) was calculated for each ontogenetic stage by calculating the average age of genes that contribute to the transcriptome (20). To compute the TAI, the expression level for each gene is multiplied by its gene age (i.e., its phylogenetic stage), and then the values for each gene in a geneset are averaged. As older phylostrata are associated with the genesis of a higher number of genes, the TAI provides more weight to genes from younger phylostrata. Altogether, lower values represent an older transcriptome age. In addition, the evolution of protein coding genes in humans and macaques was assessed by comparing their genetic sequences to their common primate ancestor via the GenEvo tool (24). From this data, the numbers of non-synonymous changes per non-synonymous sites (dN) and synonymous changes per synonymous sites (dS) were computed to calculate the dN/dS ratio to estimate the conservation of genes. Welch's *t*-test was used to compare the dN/dS ratio of the macaque and human genesets.

The functional significance of genes spatiotemporally associated with OXTR

To explore the functional significance of spatiotemporal expression patterns of genes strongly coupled with *OXTR*, a geneset including the top 100 genes with the strongest spatiotemporal correlations with *OXTR* were submitted to FUMA for annotation of genetic associations (25). Hypergeometric tests (Benjamini-Hochberg adjusted) were performed to examine if this geneset was overrepresented in GWAS from the National Human Genome Research Institute-European Bioinformatics Institute (NHGRI-EBI) GWAS catalogue (e96 2019-09-24; (26)) and biological processes from the Molecular Signatures database (MsigDB v7.0; (27)). We also calculated the top 20 correlated and anti-correlated genes between *OXTR* and the 16659

remaining genes across the lifespan, ordered by the lifespan trajectory mean using methods described above.

To assess if there was a significant difference in the association between the spatiotemporal expression of *OXTR* and genes that have been associated with psychiatric and physiological phenotypes of interest, we compared the distribution of correlation coefficients between phenotype genesets of interest against all remaining genes. We selected a range of psychiatric and psychological phenotypes that have been previously associated with oxytocin signaling dysfunction [i.e., schizophrenia (SCZ), major depressive disorder (MDD), IQ, general cognition, bipolar disorder (BD), autism spectrum disorder (ASD), and anorexia nervosa], and a set of physiological phenotypes based on results from analysis above (i.e., bone fracture, bone density, and BMI). To retrieve genesets associated with phenotypes of interest we performed genome-wide gene-based association using MAGMA (v1.08) and functional mapping of variants to genes based on expression quantitative trait loci (eQTL) via FUMA on the complete GWAS input data available from public resources (See Supplementary table 1 for details). All variants in the GWAS outside of the MHC region (chr6:28,477,797-33,448,354) were included to estimate the significance value of that gene. The eQTL approach maps SNPs to genes which are likely to affect the expression of those genes up to 1 megabase away from the SNP of interest. To determine gene expression and assess eQTL functionality of likely regulatory SNPs, we used data from the eQTL Catalogue (28), PsychENCODE (29), the xQTLServer (30), the CommonMind Consortium (31), GTEx v8 (32), and the Braineac eQTLs dataset (33). MAGMA performs multiple linear regression to obtain gene-based *p*-values and the Bonferroni-corrected significant thresholds for each phenotype is listed in Supplementary table 2. After retrieving genes, we computed Spearman's correlation coefficients to estimate the spatiotemporal relationship between *OXTR* and 16661 available genes. We then created a distribution for these correlation coefficients. Finally, genes were split into two parts, ones belonging to phenotype of interest and the remaining genes, which were superimposed for comparison. We used non-parametric Mann-Whitney U

tests to test if distributions had different medians. We adjusted reported *p*-values to the total number of brain phenotypes using a false discovery rate (FDR) threshold.

Donor-to-donor reproducibility of gene expression patterns

To calculate spatiotemporal differential stability, each of the 57 human donors were matched to their three closest three neighbors by age, with duplicates and matches with less than 4 regions in common removed, yielding a list with 93 matches. Each donor was matched 3.2 times, on average. We iterated through all the 131 matched pairs, performing the following tasks for each protein coding gene in the database to calculate spatiotemporal differential stability: 1) Extraction of gene expression for all available brain regions, 2) Calculation of Spearman's correlation coefficient, 3) Calculation of the mean Spearman's correlation coefficient among the 109 pairs.

Data and code availability

The R code to recreate our analyses and figures, along with links to the public data used in our analyses, are available at https://gitlab.com/jarek.rokicki/spatio-temporal-oxytocin/.

Results

Spatiotemporal oxytocin receptor expression in humans and macaques

Our analysis revealed that *OXTR* expression across the brain in humans begins to accelerate just before birth, with a peak level of expression occurring during early childhood (Fig. 1a), consistent with previously reported *OXTR* receptor binding temporal patterns from the ventral pallidum (11). Regional analyses demonstrated increased *OXTR* expression in the mediodorsal nucleus of the thalamus during early childhood (Fig. 1b) and in the cerebellar cortex and medial prefrontal cortex in later childhood. During adulthood, expression increased

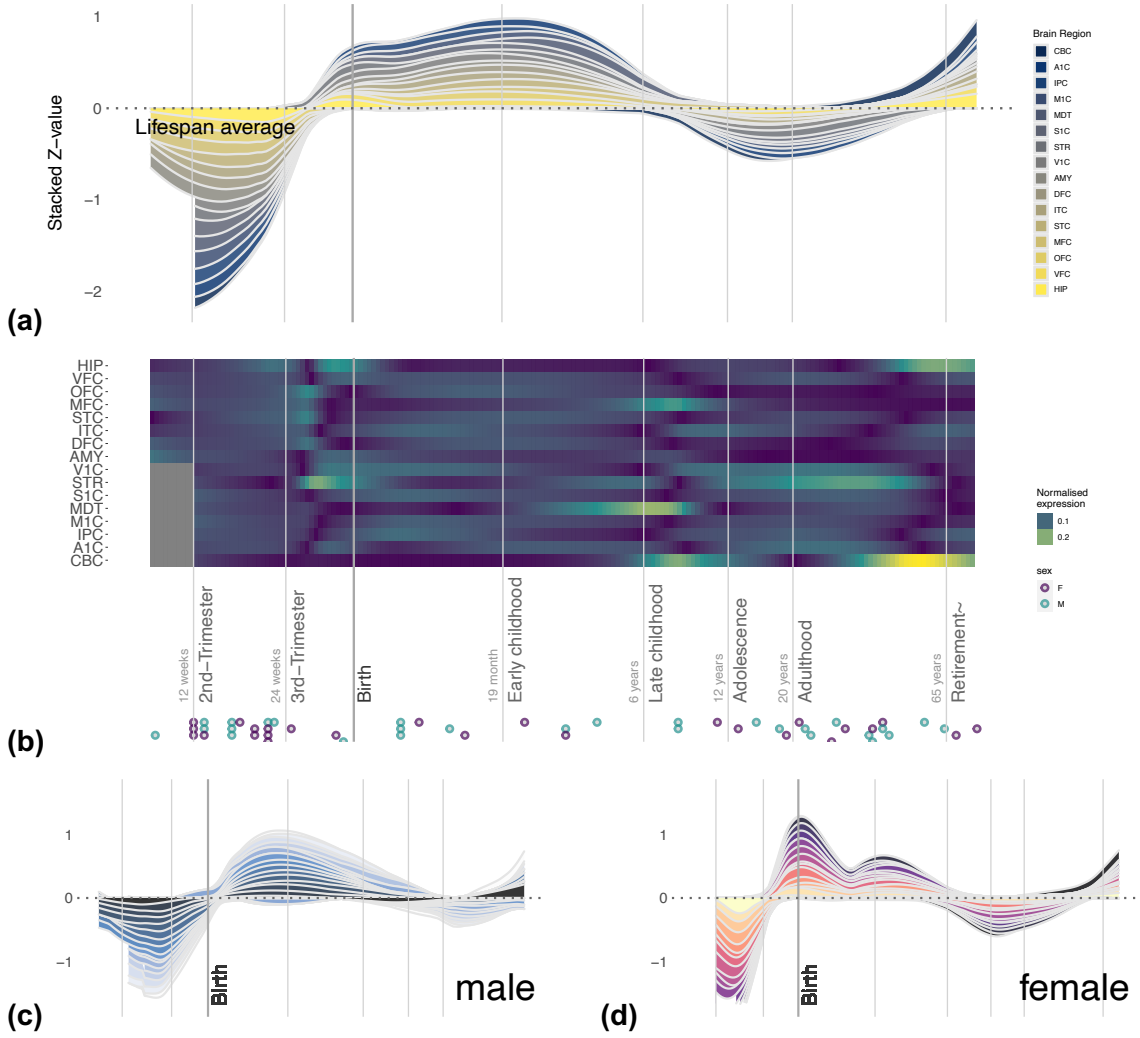

Figure 1. *OXTR* gene expression in sixteen regions of the human brain across different developmental phases. (a) The ribbon plot illustrates normalized gene expression compared to the lifespan average, with expression of individual brain regions stacked. The stacked Z-value is scaled to the number of regions (sixteen). **(b)** The heat plot illustrates gene expression across sixteen brain regions, normalized for each brain region across the lifespan. There is increased *OXTR* expression in the MFC, S1C, and CBC during late childhood, and increased expression in the STR and V1C during adulthood (see methods for a key to brain regions). Each individual donor and their sex are shown at the bottom of the panel. Time is presented using a log10 scale in both panels. Also presented are ribbon plots with data from only males **(c)** and females **(d)**, with each panel illustrating normalized gene expression compared to the lifespan average. Males demonstrated a stronger early childhood peak compared to females, who demonstrated the highest OXTR expression just after birth.

in the striatum. Males exhibited a stronger early childhood peak in *OXTR* expression and more pronounced differentiation within brain regions (Figs. 1c and 1d; see Supplementary Figure 1 for greater detail). Expression patterns of *CD38*, which regulates oxytocin secretion, and the structural gene for oxytocin (*OXT*) are presented in Supplementary figures 2 and 3.

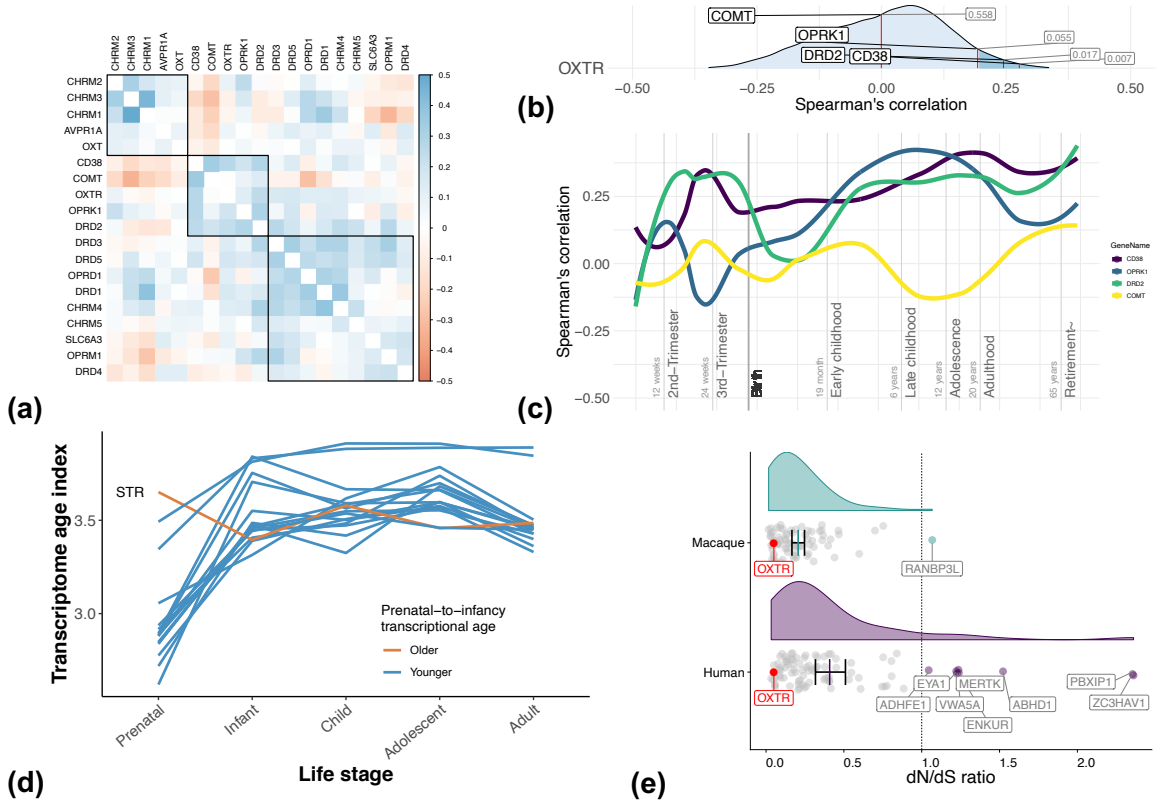

Figure 2. *OXTR* spatiotemporal co-expression and the evolution of *OXTR* co-expression modules. (a) The spatiotemporal correlation between *OXTR* and a selection of oxytocinergic, dopaminergic, muscarinic acetylcholine, and opioid pathway genes. *OXTR* was part of a five-gene spatiotemporal co-expression module with *DRD2*, *COMT*, *OPRK1*, and *CD38*. **(b)** The percentage rank of the spatiotemporal relationship between *OXTR* and *DRD2*, *COMT*, *OPRK1*, and *CD38*, compared with to the spatiotemporal relationship between OXTR and all protein coding genes (n = 16659). Both *DRD2* and *CD38* were among with the top 5% of correlations (marked in dark blue). **(c)** The lifespan stability of the spatiotemporal correlation between *OXTR* and *DRD2*, *COMT*, *OPRK1*, *CD38*. **(d)** The transcriptional age of a gene co-expression module comprising *OXTR* and the 100 genes with the strongest spatiotemporal co-expression with *OXTR* across the lifespan in sixteen brain regions (see methods), with a smaller transcriptional age index representing an older transcriptome. Analysis suggested an older transcriptional age in infancy compared to the prenatal stage across the brain, except for the striatum (STR). **(e)** The top 100 gene module was more highly conserved in the macaque genome compared to the human genome (p = 0.0001), however, in both species *OXTR* (marked in red) is highly conserved. Several genes from this geneset had undergone positive selection in humans (i.e., dN/dS ratio values > 1).

Lifespan correlation between genes

Hierarchical clustering identified a set of genes with particularly strong correlations for the spatiotemporal expression pattern of *OXTR*, which included *CD38*, COMT, *OPRK1*, and *DRD2* (Fig. 2a). Figure 2b shows the distribution of the spatiotemporal correlations between

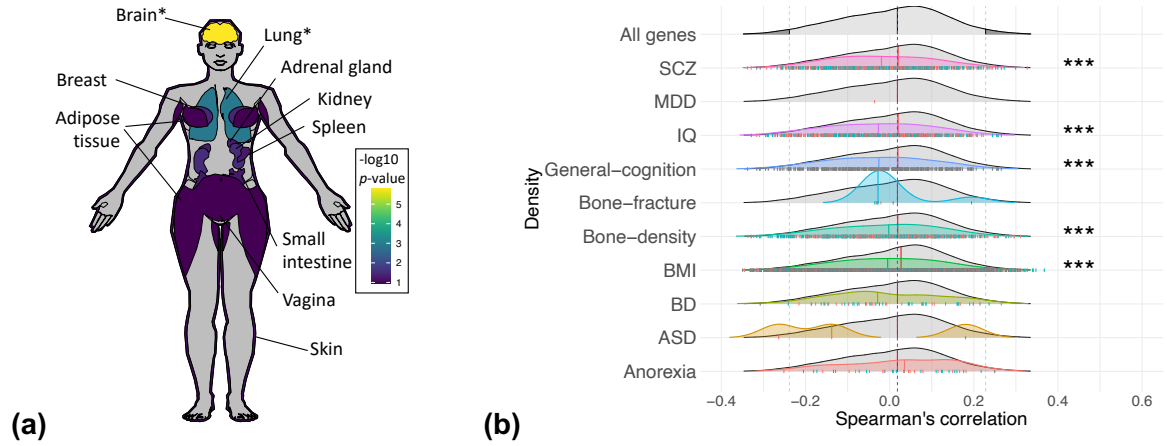

Figure 3. Networks of genes with strong spatiotemporal couplings with *OXTR* are enriched in brain and lung tissue, body composition phenotypes, and psychological phenotypes. (a) Top ten highest levels of differential expression in human tissue types of a geneset containing the top 100 genes correlated with *OXTR*. -log10 *p*-values for upregulation of this geneset in various tissue types, represent the probability of the hypergeometric tests. See Supplementary figure 7 for a list of results with 30 tissue types. *$p < 0.05$ (Bonferroni corrected). **(b)** Comparisons between the correlation of *OXTR* with genes related to disorders based on eQTL mapping and phenotypes and the correlation of *OXTR* with remaining genes. Vertical dashes in each distribution represent genes correlation between genes involved in phenotype and *OXTR*. Blue notches indicate risk increasing alleles which increase the expression of the gene, red notches indicate when risk increasing alleles decrease the expression of the gene, and grey notches indicate when direction is unknown, under respective distributions. ***$p < 0.001$ (FDR corrected).

OXTR and all remaining genes, marking the location of the genes clustered with *OXTR*. This analysis revealed that *DRD2* was among the top 1.7% of all correlated genes (total number of genes = 16660), and this correlation remained relatively stable from early childhood onward (Fig. 2c).

The evolutionary origin of OXTR and spatiotemporally related genes

As we observed in our human data analysis, a late-prenatal acceleration of *OXTR* expression was observed in macaques, however, there was no evidence of an early childhood peak (Supplementary Fig. 4). *DRD2* was included in a cluster of genes with high spatiotemporal correlations with *OXTR*, but the relationship between *OXTR* and *DRD2* was only in the top 81.7% of correlations of *OXTR* with all other protein coding genes (Supplementary Fig. 5).

Table 1. Top 20 correlated and anti-correlated genes with *OXTR* across lifespan

	Top correlated			Top anti-correlated		
Rank	Gene	Trajectory	Arithmetic	Gene	Trajectory	Arithmetic
1	FGFR3	0.368	0.365	DEPDC5	-0.381	-0.365
2	GRAMD1C	0.358	0.363	CACNA1A	-0.368	-0.382
3	C1orf88	0.356	0.358	KLC2	-0.363	-0.373
4	NTSR2	0.35	0.318	KCNC3	-0.363	-0.313
5	INHBB	0.348	0.328	C2CD3	-0.361	-0.319
6	CXorf59	0.343	0.348	HDAC8	-0.359	-0.345
7	KCNN3	0.341	0.336	CTCF	-0.349	-0.3
8	DIRAS3	0.34	0.286	MAP3K12	-0.347	-0.356
9	STON2	0.338	0.345	MICAL2	-0.345	-0.313
10	RDH10	0.335	0.338	APBA2	-0.345	-0.285
11	AGXT2L1	0.328	0.301	MORC2	-0.343	-0.334
12	SIL1	0.327	0.293	NOVA1	-0.341	-0.318
13	HRSP12	0.326	0.316	NFIX	-0.34	-0.321
14	GLUD1	0.323	0.309	KCNJ3	-0.338	-0.333
15	GNG12	0.323	0.32	KDM5C	-0.337	-0.345
16	PBXIP1	0.321	0.304	SEMA4C	-0.333	-0.315
17	RUNX3	0.319	0.289	EPS15L1	-0.332	-0.33
18	F3	0.317	0.312	TMEM25	-0.33	-0.325
19	ACSBG1	0.317	0.303	DHX8	-0.33	-0.307
20	GJA1	0.316	0.301	ADAM11	-0.329	-0.275

Two approaches for this analysis are presented. "Trajectory" represents a mean correlation across the lifespan trajectory, in which each life period receives an equal weighting. "Arithmetic" represents the mean of individual correlations between donors, in which each donor is weighted equally.

A phylostratigraphic analysis revealed that most genes in a module containing genes with the 100 strongest spatiotemporal correlations with *OXTR* are evolutionary ancient, appearing among the first three phylostrata (Supplementary Fig. 6). In particular, the ancestor of *OXTR* first emerged in the Eumetazoa phylostrata. A transcriptional age index (TAI) was calculated for sixteen brain regions across five ontogenetic stages, for which lower TAI values represent an older transcriptome. For all brain regions except the striatum (STR), the transcriptome of the *OXTR* top 100 geneset was older during the prenatal stage, compared to later stages (Fig. 2d). This suggests that genes in this transcriptome that are highly expressed from infancy onward evolved at a faster rate compared to genes that are highly expressed prenatally, for most brain regions we investigated.

Next, we calculated the dN/dS ratio to assess whether genes in the top 100 geneset had experienced positive selection (dN/dS > 1), negative selection (dN/dS < 1), or if they have been evolving neutrally (dN/dS ~ 1), in both the human and macaque genome (24). While *OXTR* is highly conserved in both humans and macaques, the total geneset on average had a significantly higher dN/dS ratio in humans, compared to macaques [t = 3.96 (123.3), p = 0.0001, d = 0.6; Fig. 2e]. This analysis also revealed that a number of genes show specific divergence in humans (i.e., positive selection), but not macaques, in which they are under selective constraint (*ADHFE1*, *EYA1*, *MERTK*, *VWA5A*, *ENKUR*, *ABHD1*, *PBXIP1*, and *ZC3HAV1*).

The functional significance of spatiotemporally expression pattern

Annotating the associations of a geneset including 100 genes with the strongest spatiotemporal associations with *OXTR* revealed enrichment in GWAS-derived genes for bone fracture in osteoporosis ($p = 8.923 \times 10^{-3.}$) In addition, there was enrichment with genes associated with age-related macular degeneration GWAS ($p = 8.293 \times 10^{-3}$), as well as gene ontology genesets associated with reproduction ($p = 5.83 \times 10^{-3}$) and penile erection ($p = 5.83 \times 10^{-3}$). We also examined the enrichment of this geneset in thirty tissue types across the body using the GTEx database (version 8; (32)) in FUMA, discovering up-regulated differentially expressed genes in brain and lung tissue (p > 0.05, Bonferroni corrected; Fig. 3a; Supplementary Fig. 7). The twenty genes showing the strongest spatiotemporal correlations with *OXTR* gene expression are presented in Table 1. Some of the most positively correlated genes have been associated with bone mass regeneration (*FGFR3*) (34,35), bone density (*DIRAS3*) (26), glucose (*NTSR2*) (36) and insulin allostasis (*GLUD1*) (37), and hypothalamic (*INHBB*) secretion (38). Some of the strongest negatively correlated genes have been associated with body mass index (*MAP3K12*, *MORC2*) (26) and bone density (*CTCF*,

MORC2) (26). Notably, some of the highest correlated genes in this spatiotemporal analysis (e.g., *NTSR2*, *GLUD1*, *SRPK1*, *MTCL1*, *KCNJ3*, *PAK7*, *THBS4*, *HEYL*, *ZC3HAV1*) were also among the highest correlated in a previous analysis of *OXTR* expression in human adults using a different gene expression dataset (6).

To examine the relationship between the spatiotemporal expression of *OXTR* and genes that have been associated with psychological and physiological phenotypes of interest, we extracted phenotype genesets by using expression quantitative trait loci (eQTL) mapping of GWAS data (Supplementary table 1). To determine specificity, we compared these results with the relationship between spatiotemporal expression of *OXTR* and genes *not* included in the phenotype geneset of interest. The correlations with the genesets of interest and the background genes were both plotted as density distributions and non-parametric Mann-Whitney U tests were performed to compare the distributions. There was a significantly lower density median for the relationship of *OXTR* with genesets enriched in schizophrenia, IQ, general cognition, bone density, and BMI, compared to the median of the density distribution with background genes, adjusting tests via a false discovery rate threshold ($p < 0.001$; Fig. 3b; Supplementary Table 3). Genes related to phenotypes falling within top or bottom 2.5% of *OXTR* correlation's distribution are provided in Supplementary tables 4 and 5. Similar results were found using a MAGMA analysis (Supplementary Fig. 8; Supplementary Tables 6, 7, 8).

Donor-to-donor reproducibility of gene expression patterns

As the number of donor samples in these analyses is relatively small, it is important to confirm the stability of spatiotemporal gene expression patterns from donor-to-donor to make meaningful inferences beyond the sample. Thus, we calculated a measure of donor-to-donor spatiotemporal differential stability. Genes with a differential stability score in the top 50% of all genes are considered to be conserved (39). Previous work has demonstrated that genes with high differential stability have strong biological relevance (39) and that *OXTR* expression

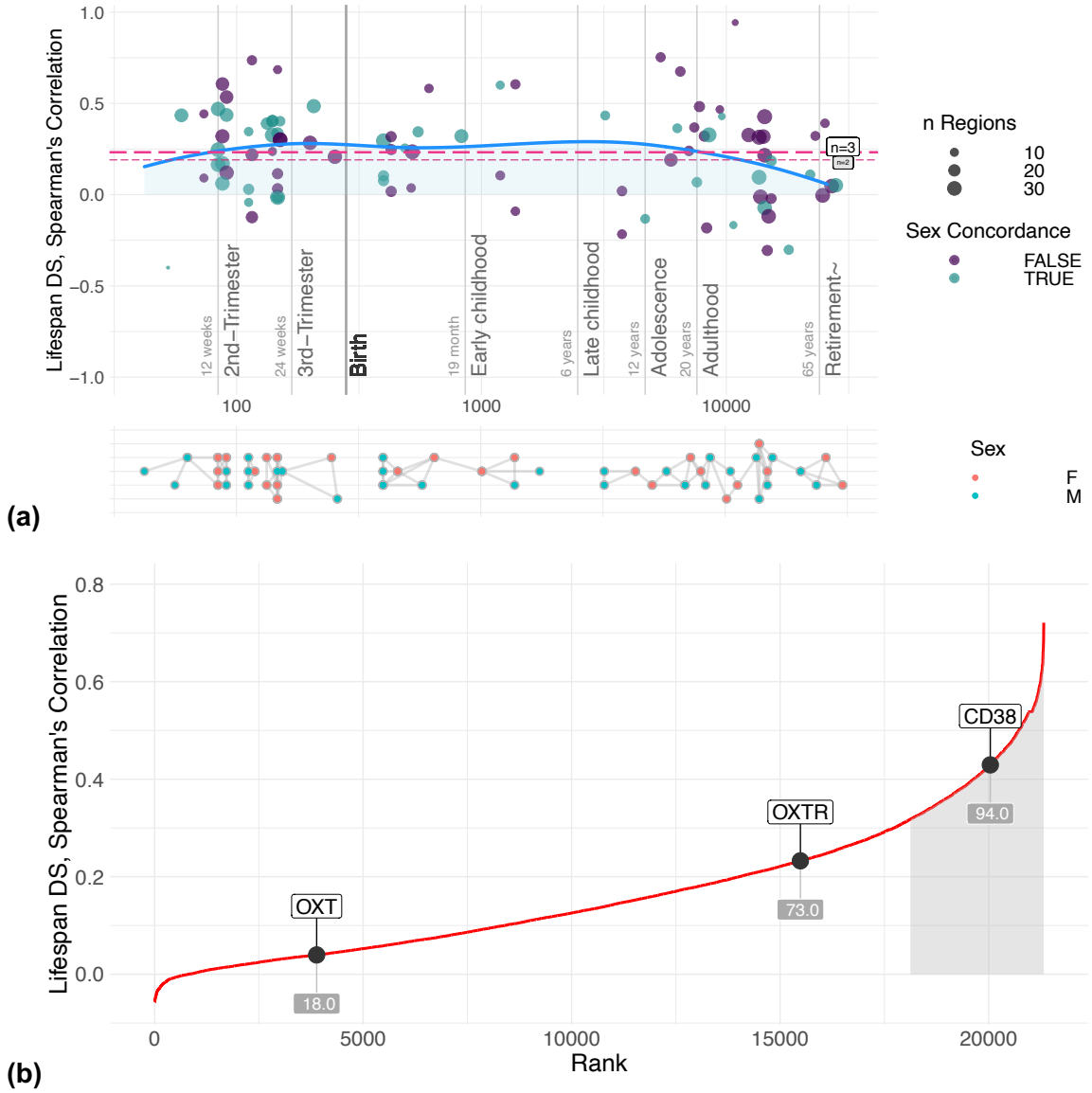

388 **Figure 4. Differential stability for *OXTR*, *CD38*, and *OXT* across development. (a)** The differential stability of
389 *OXTR* is relatively constant across the lifespan, with a modest dip during adulthood. The blue line represents
390 lifespan trajectory and the dashed horizontal red lines illustrate the mean of all points (long dashes = 3 pair
391 comparisons; short dashes = 4 pair comparisons). Purple dots show the correlation between two donors of the
392 same sex, whereas turquoise dots show the correlations of opposite sexes. The size of the dots corresponds to
393 the number of brain regions. The bottom section illustrates a map of donor comparisons, where pairs used for
394 differential stability estimation are connected with edges. **(b)** The differential stability of *OXTR*, *CD38*, and *OXT*
395 were compared against 21,323 genes, across development. Genes in the top 15% of differential stability values
396 are shaded in light grey. Both *CD38* and *OXTR* can be considered to be highly conserved as their scores are in
397 the top 50% (39).

398

399 patterns have high person-to-person stability in an adult sample (6). We found that both *OXTR*
400 and *CD38* were among the top 30% of all protein coding genes in terms of spatiotemporal

differential stability (Fig. 4). This indicates that expression patterns of these genes are relatively stable in donors of a similar age. Differential stability of *OXTR* expression across development also remains relatively constant across macaque development (Supplementary Fig. 9).

Discussion

Here we characterized spatiotemporal gene expression patterns in human brain tissue, revealing increased *OXTR* expression during early childhood and a strong association between the spatiotemporal expression of *OXTR* and a key gene regulating dopaminergic signaling (*DRD2*). These features are conserved across individuals and appear to have emerged recently in human evolutionary history, as these gene expression patterns were not observed in a macaque sample. Moreover, we found that a geneset including genes with the strongest 100 associations with the *OXTR* spatiotemporal expression pattern is enriched in schizophrenia, IQ, general cognition, osteoporosis, reproductive processes, and BMI.

Our analyses revealed a distinct pattern of *OXTR* expression in the human brain across the lifespan, with an *OXTR* expression peak during childhood. This childhood peak was especially pronounced in males, which may contribute to reported sex differences in neurodevelopmental disorder diagnoses (40,41). While the production and distribution of oxytocin in the brain is relatively similar across mammalian species (42), the location of oxytocin receptors in the brain varies between mammalian species both spatially (43,44) and temporally (18). Indeed, differences in temporal expression peaks may reveal differing critical periods for experience-dependent development mediated by oxytocin signaling (45). For example, peak *OXTR* expression in mice occurs during the postnatal period (46,47), which has also been shown to be a critical period for oxytocin-mediated cortical plasticity (48). Altogether, our observation of increased expression during early childhood highlights oxytocin's role during this critical life period in humans (11).

We have previously demonstrated the strong co-expression of *OXTR* and dopaminergic signaling genes and the link between the *OXTR* expression pattern and brain regions associated with learning in the adult human brain (6). The strong spatiotemporal correlation between *OXTR* and *DRD2* gene expression observed in the present study suggests that the oxytocin system works synergistically throughout development with the dopaminergic signaling to support learning (49), especially during critical developmental periods (2). We also demonstrated that *OXTR* is evolutionarily ancient, with its ancestor emerging around the Bilateria phylostrata during which basic nervous systems first appeared (50). However, the oxytocin system's integration with other signaling systems, and ultimately its purpose, seems to have shifted over time in response to novel environmental pressures (42). The increased integration of the oxytocin signaling system with the dopaminergic system in humans, compared to macaques, supports the critical importance of social learning in humans during early childhood (51).

In terms of the functional relevance of the *OXTR* spatiotemporal expression pattern, we found that this was highly correlated with a set of genes enriched for bone fracture. Moreover, several individual genes that were strongly associated with *OXTR* expression patterns have also been linked to bone integrity (i.e., *FGFR3*, *DIRAS3*, *CTCF* and *MORC2*). This is certainly not the first time the link between oxytocin signaling and bone remodeling has been highlighted (e.g., 52), however, the present results suggest that gene-gene co-expression in the brain may contribute to this association. Intriguingly, bone remodeling issues have been identified in autism (53), which has been associated with oxytocin signaling dysfunction (41), and oxytocin receptor knockout mice have been shown to develop osteoporosis (54). Moreover, peripheral oxytocin levels have been linked to bone mineral density in men with hypopituitarism (55) and post-menopausal women (56). Leptin release has been proposed as the primary central mediator of bone remodeling (57), but our results suggest that oxytocin may also play a critical role in this process. Although speculative, this

finding points to a possible pleiotropic effect of oxytocin dysfunction on social difficulties and bone remodeling, which warrants further investigation.

There are two limitations to the study worth noting. First, the donor sample sizes for both humans and macaques were relatively small. However, high differential stability values demonstrate that *OXTR* expression patterns were relatively stable from donor-to-donor in both human and macaque samples across the lifespan. Moreover, genes with high spatiotemporal co-expression with *OXTR* in the present study were also found to be highly co-expressed in our previous study in human adults, which used a different dataset for analysis (6). Second, we used transcriptome data as a proxy for gene expression density (19). While other methods directly measure *OXTR* expression density (e.g., competitive-binding receptor autoradiography), it is not practical to assess co-expression for more than a few receptors at a time using such approaches. While transcriptome measures are a less direct method, this facilitates the analysis of gene-gene co-expression patterns for thousands of receptor and non-receptor genes, which can help unravel the functional organization of the brain (39), for which oxytocin signaling was the focus in the present paper.

Here we provide evidence for distinct *OXTR* expression patterns that are enriched in psychological and body composition processes across development. These findings are consistent with the allostatic theory of oxytocin, which uniquely accounts for oxytocin's effects on both behavioral and non-behavioral traits and highlights the importance of oxytocin signaling function changes across the lifespan to adapt to shifting environmental challenges (2). By mapping the spatiotemporal *OXTR* gene expression pattern, identifying co-expressed genes, and better characterizing the evolutionary history of this pattern we provide evidence that oxytocin signaling is implicated in a broad suite of psychological and physiological functions across the lifespan, and that this supporting role of the oxytocin system might be unique to humans.

Acknowledgements

This research was funded by the Research Council of Norway (301767), the Novo Nordisk Foundation (NNF16OC0019856), and the ERA-Net Cofund through the ERA PerMed project "IMPLEMENT".

Competing interests

The authors have no competing interests to disclose.

References

1. Jurek B, Neumann ID (2018): The oxytocin receptor: from intracellular signaling to behavior. *Physiol Rev* 98: 1805–1908.

2. Quintana DS, Guastella AJ (2020): An allostatic theory of oxytocin. *Trends Cogn Sci* 24: 515–528.

3. Busnelli M, Chini B (2018): Molecular Basis of Oxytocin Receptor Signalling in the Brain: What We Know and What We Need to Know. *Curr Top Behav Neurosci* 35: 3–29.

4. Keebaugh AC, Barrett CE, Laprairie JL, Jenkins JJ, Young LJ (2015): RNAi knockdown of oxytocin receptor in the nucleus accumbens inhibits social attachment and parental care in monogamous female prairie voles. *Soc Neurosci* 10: 561–570.

5. Nishimori K, Takayanagi Y, Yoshida M, Kasahara Y, Young LJ, Kawamata M (2008): New aspects of oxytocin receptor function revealed by knockout mice: sociosexual behaviour and control of energy balance ((I. D. Neumann & R. Landgraf, editors)). *Prog Brain Res* 170: 79–90.

6. Quintana DS, Rokicki J, van der Meer D, Alnæs D, Kaufmann T, Córdova-Palomera A, *et al.* (2019): Oxytocin pathway gene networks in the human brain. *Nat Commun* 10: 668.

7. Lee MR, Sheskier MB, Farokhnia M, Feng N, Marenco S, Lipska BK, Leggio L (2018): Oxytocin receptor mRNA expression in dorsolateral prefrontal cortex in major psychiatric disorders: A human post-mortem study. *Psychoneuroendocrinology* 96: 143–147.

8. Uhrig S, Hirth N, Broccoli L, von Wilmsdorff M, Bauer M, Sommer C, *et al.* (2016): Reduced oxytocin receptor gene expression and binding sites in different brain regions in schizophrenia: A post-mortem study. *Schizophr Res*. https://doi.org/10.1016/j.schres.2016.04.019

9. Kang HJ, Kawasawa YI, Cheng F, Zhu Y, Xu X, Li M, *et al.* (2011): Spatiotemporal transcriptome of the human brain. *Nature* 478: 483–489.

10. Kim DR, Bale TL, Epperson CN (2015): Prenatal programming of mental illness: current understanding of relationship and mechanisms. *Curr Psychiatry Rep* 17: 5.

11. Freeman SM, Palumbo MC, Lawrence RH, Smith AL, Goodman MM, Bales KL (2018): Effect of age and autism spectrum disorder on oxytocin receptor density in the human basal forebrain and midbrain. *Transl Psychiatry* 8: 1–11.

12. Boer GJ, Swaab DF, Uylings HBM, Boer K, Buijs RM, Velis DN (1980): Neuropeptides in Rat Brain Development. In: McConnell PS, Boer GJ, Romijn HJ, Van De Poll NE, Corner MA, editors. *Progress in Brain Research*, vol. 53. Elsevier, pp 207–227.

13. Swaab DF (1995): Development of the human hypothalamus. *Neurochem Res* 20: 509–519.

14. Pedersen CA, Boccia ML (2002): Oxytocin links mothering received, mothering bestowed and adult stress responses. *Stress Amst Neth* 5: 259–267.

15. Winslow JT, Noble PL, Lyons CK, Sterk SM, Insel TR (2003): Rearing effects on cerebrospinal fluid oxytocin concentration and social buffering in rhesus monkeys. *Neuropsychopharmacology* 28: 910–918.

16. Francis DD, Champagne FC, Meaney MJ (2000): Variations in maternal behaviour are associated with differences in oxytocin receptor levels in the rat. *J Neuroendocrinol* 12: 1145–1148.

17. Heim C, Young LJ, Newport DJ, Mletzko T, Miller AH, Nemeroff CB (2009): Lower CSF oxytocin concentrations in women with a history of childhood abuse. *Mol Psychiatry* 14: 954–958.

18. Vaidyanathan R, Hammock EA (2017): Oxytocin receptor dynamics in the brain across development and species. *Dev Neurobiol* 77: 143–157.

19. Young LJ, Muns S, Wang Z, Insel TR (1997): Changes in oxytocin receptor mRNA in rat brain during pregnancy and the effects of estrogen and interleukin-6. *J Neuroendocrinol* 9: 859–865.

20. Domazet-Lošo T, Tautz D (2010): A phylogenetically based transcriptome age index mirrors ontogenetic divergence patterns. *Nature* 468: 815–818.

21. Hawrylycz M, Lein ES, Guillozet-Bongaarts AL, Shen EH, Ng L, Miller JA, *et al.* (2012): An anatomically comprehensive atlas of the adult human brain transcriptome. *Nature* 489: 391.

22. Domazet-Lošo T, Tautz D (2008): An Ancient Evolutionary Origin of Genes Associated with Human Genetic Diseases. *Mol Biol Evol* 25: 2699–2707.

23. Drost H-G, Gabel A, Liu J, Quint M, Grosse I (2018): myTAI: evolutionary transcriptomics with R. *Bioinformatics* 34: 1589–1590.

24. Dumas G, Malesys S, Bourgeron T (2021): Systematic detection of brain protein-coding genes under positive selection during primate evolution and their roles in cognition. *Genome Res* 31: 484–496.

25. Watanabe K, Taskesen E, Bochoven A, Posthuma D (2017): Functional mapping and annotation of genetic associations with FUMA. *Nat Commun* 8: 1826.

26. MacArthur J, Bowler E, Cerezo M, Gil L, Hall P, Hastings E, *et al.* (2017): The new NHGRI-EBI Catalog of published genome-wide association studies (GWAS Catalog). *Nucleic Acids Res* 45: D896–D901.

27. Liberzon A, Subramanian A, Pinchback R, Thorvaldsdóttir H, Tamayo P, Mesirov JP (2011): Molecular signatures database (MSigDB) 3.0. *Bioinformatics* 27: 1739–1740.

28. Kerimov N, Hayhurst JD, Peikova K, Manning JR, Walter P, Kolberg L, *et al.* (2021): eQTL Catalogue: a compendium of uniformly processed human gene expression and splicing QTLs. *bioRxiv* 2020.01.29.924266.

29. Akbarian S, Liu C, Knowles JA, Vaccarino FM, Farnham PJ, Crawford GE, *et al.* (2015): The PsychENCODE project. *Nat Neurosci* 18: 1707–1712.

30. Ng B, White CC, Klein H-U, Sieberts SK, McCabe C, Patrick E, *et al.* (2017): An xQTL map integrates the genetic architecture of the human brain's transcriptome and epigenome. *Nat Neurosci* 20: 1418–1426.

31. Hoffman GE, Bendl J, Voloudakis G, Montgomery KS, Sloofman L, Wang Y-C, *et al.* (2019): CommonMind Consortium provides transcriptomic and epigenomic data for Schizophrenia and Bipolar Disorder. *Sci Data* 6: 180.

562 32. Aguet F, Brown AA, Castel SE, Davis JR, He Y, Jo B, *et al.* (2017): Genetic effects on gene
563 expression across human tissues. *Nature* 550: 204–213.
564 33. Ramasamy A, Trabzuni D, Guelfi S, Varghese V, Smith C, Walker R, *et al.* (2014): Genetic
565 variability in the regulation of gene expression in ten regions of the human brain. *Nat*
566 *Neurosci* 17: 1418–1428.
567 34. Valverde-Franco G, Liu H, Davidson D, Chai S, Valderrama-Carvajal H, Goltzman D, *et al.* (2004):
568 Defective bone mineralization and osteopenia in young adult FGFR3−/− mice. *Hum Mol*
569 *Genet* 13: 271–284.
570 35. Mugniery E, Dacquin R, Marty C, Benoist-Lasselin C, de Vernejoul M-C, Jurdic P, *et al.* (2012): An
571 activating Fgfr3 mutation affects trabecular bone formation via a paracrine mechanism
572 during growth. *Hum Mol Genet* 21: 2503–2513.
573 36. Mazella J, Béraud-Dufour S, Devader C, Massa F, Coppola T (2012): Neurotensin and its receptors
574 in the control of glucose homeostasis. *Front Endocrinol* 3. https://doi.org/10/gft367
575 37. Tanizawa Y, Nakai K, Sasaki T, Anno T, Ohta Y, Inoue H, *et al.* (2002): Unregulated Elevation of
576 Glutamate Dehydrogenase Activity Induces Glutamine-Stimulated Insulin Secretion:
577 Identification and Characterization of a GLUD1 Gene Mutation and Insulin Secretion Studies
578 With MIN6 Cells Overexpressing the Mutant Glutamate Dehydrogenase. *Diabetes* 51: 712–
579 717.
580 38. Ying S-Y (1987): Inhibins and Activins: Chemical Properties and Biological Activity. *Proc Soc Exp*
581 *Biol Med* 186: 253–264.
582 39. Hawrylycz M, Miller JA, Menon V, Feng D, Dolbeare T, Guillozet-Bongaarts AL, *et al.* (2015):
583 Canonical genetic signatures of the adult human brain. *Nat Neurosci* 18: 1832.
584 40. Ferri SL, Abel T, Brodkin ES (2018): Sex Differences in Autism Spectrum Disorder: a Review. *Curr*
585 *Psychiatry Rep* 20: 9.
586 41. Guastella AJ, Hickie IB (2016): Oxytocin treatment, circuitry and autism: a critical review of the
587 literature placing oxytocin into the autism context. *Biol Psychiatry* 79: 234–242.

588 42. Knobloch HS, Grinevich V (2014): Evolution of oxytocin pathways in the brain of vertebrates.
589 *Front Behav Neurosci* 8: 31.
590 43. Leung CH, Abebe DF, Earp SE, Goode CT, Grozhik AV, Mididoddi P, Maney DL (2011): Neural
591 distribution of vasotocin receptor mRNA in two species of songbird. *Endocrinology* 152:
592 4865–4881.
593 44. Freeman SM, Young LJ (2016): Comparative Perspectives on Oxytocin and Vasopressin Receptor
594 Research in Rodents and Primates: Translational Implications. *J Neuroendocrinol* 28.
595 https://doi.org/10.1111/jne.12382
596 45. Hammock E (2015): Developmental perspectives on oxytocin and vasopressin.
597 *Neuropsychopharmacology* 40: 24.
598 46. Mitre M, Marlin BJ, Schiavo JK, Morina E, Norden SE, Hackett TA, *et al.* (2016): A Distributed
599 Network for Social Cognition Enriched for Oxytocin Receptors. *J Neurosci* 36: 2517–2535.
600 47. Hammock E, Levitt P (2013): Oxytocin receptor ligand binding in embryonic tissue and postnatal
601 brain development of the C57BL/6J mouse. *Front Behav Neurosci* 7: 195.
602 48. Zheng J-J, Li S-J, Zhang X-D, Miao W-Y, Zhang D, Yao H, Yu X (2014): Oxytocin mediates early
603 experience–dependent cross-modal plasticity in the sensory cortices [no. 3]. *Nat Neurosci*
604 17: 391–399.
605 49. Love TM (2014): Oxytocin, motivation and the role of dopamine. *Pharmacol Biochem Behav* 119:
606 49–60.
607 50. Kelava I, Rentzsch F, Technau U (2015): Evolution of eumetazoan nervous systems: insights from
608 cnidarians. *Philos Trans R Soc B Biol Sci* 370: 20150065.
609 51. Nielsen M (2012): Imitation, pretend play, and childhood: Essential elements in the evolution of
610 human culture? *J Comp Psychol* 126: 170–181.
611 52. Copland JA, Ives KL, Simmons DJ, Soloff MS (1999): Functional Oxytocin Receptors Discovered In
612 Human Osteoblasts. *Endocrinology* 140: 4371–4374.

613 53. Hediger ML, England LJ, Molloy CA, Yu KF, Manning-Courtney P, Mills JL (2008): Reduced Bone
614 Cortical Thickness in Boys with Autism or Autism Spectrum Disorder. *J Autism Dev Disord* 38:
615 848–856.
616 54. Tamma R, Colaianni G, Zhu L, DiBenedetto A, Greco G, Montemurro G, *et al.* (2009): Oxytocin is
617 an anabolic bone hormone. *Proc Natl Acad Sci* 106: 7149–7154.
618 55. Aulinas A, Guarda FJ, Yu EW, Haines MS, Asanza E, Silva L, *et al.* (2021): Lower Oxytocin Levels
619 Are Associated with Lower Bone Mineral Density and Less Favorable Hip Geometry in
620 Hypopituitary Men. *Neuroendocrinology* 111: 87–98.
621 56. Breuil V, Panaia-Ferrari P, Fontas E, Roux C, Kolta S, Eastell R, *et al.* (2014): Oxytocin, a New
622 Determinant of Bone Mineral Density in Post-Menopausal Women: Analysis of the OPUS
623 Cohort. *J Clin Endocrinol Metab* 99: E634–E641.
624 57. Ducy P, Amling M, Takeda S, Priemel M, Schilling AF, Beil FT, *et al.* (2000): Leptin Inhibits Bone
625 Formation through a Hypothalamic Relay: A Central Control of Bone Mass. *Cell* 100: 197–
626 207.
627
628